Flexible and Printed Electronics

Printable stretchable interconnects

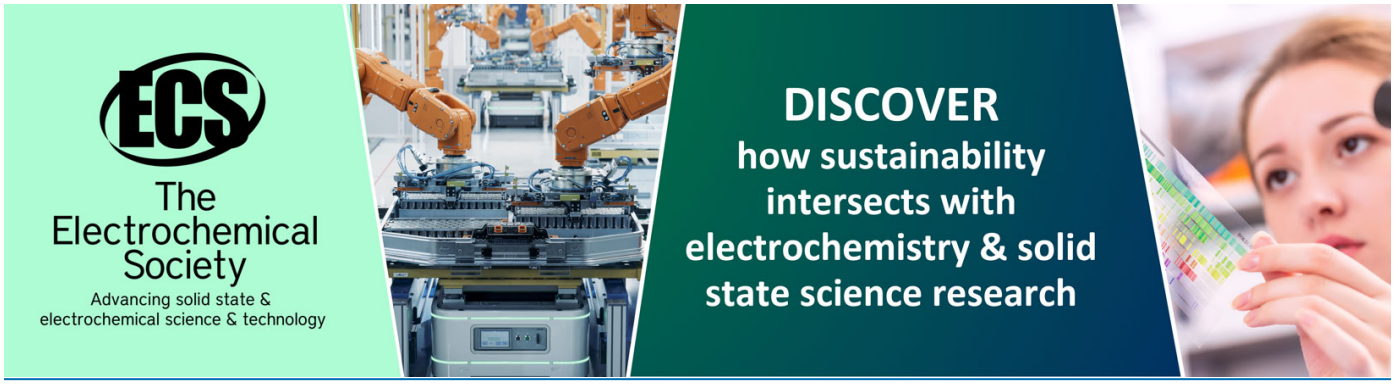

Flexible and Printed Electronics

OPEN ACCESS

RECEIVED
4 October 2016

ACCEPTED FOR PUBLICATION
19 January 2017

PUBLISHED
13 March 2017

TOPICAL REVIEW

Printable stretchable interconnects

Wenting Dang[1,2], **Vincenzo Vinciguerra**[3], **Leandro Lorenzelli**[2] **and Ravinder Dahiya**[1]

[1] Bendable Electronics and Sensing Technologies Group, School of Engineering, University of Glasgow, G128QQ, United Kingdom
[2] Microsystem Technology Research Unit, CMM, Fondazione Bruno Kessler, Trento, 38123, Italy
[3] ST Microelectronics, Catania, Italy

E-mail: Ravinder.Dahiya@glasgow.ac.uk

Keywords: stretchable electronics, interconnects, stretchable interconnects, printed sensors, nanocomposites

Abstract

This article presents recent progress and a comprehensive overview of stretchable interconnects based on printable nanocomposites. Nanocomposite-based inks for printed stretchable interconnects have been categorized according to dispersed filler materials. They comprise of carbon-based fillers and metal-based fillers. Benefits in terms of excellent electrical performance and elastic properties make nanocomposites the ideal candidates for stretchable interconnect applications. Deeper analysis of nanocomposites-based stretchable interconnects includes the correlation between the size of fillers, percolation ratio, maximum electrical conductivity and mechanical elasticity. The key trends in the field have been highlighted using curve fitting methods on large data collected from the literature. Furthermore, a wide variety of applications for stretchable interconnects are presented.

1. Introduction

Recent years have witnessed a paradigm shift in the electronics industry towards the development of flexible and stretchable electronics. Development of flexible and stretchable devices has enabled new pathways and interaction mechanisms for applications such as wearable electronics [1, 2], consumer electronics [3], electronic skin (E-skin) [4, 5] and robotics [6–8], etc. However, realization of such devices with traditional materials such as silicon is a challenge owing to their intrinsic properties such as brittleness that limit their ability to stretch or bend [9, 10]. Although recent studies on silicon micro/nanostructures [11–14] and ultra-thin chips [15, 16] have demonstrated the feasibility of silicon-based flexible electronics. In this regard, stretchable interconnects are interesting as they can provide traditional rigid electronic systems an extra degree of freedom while retaining the performance of original rigid devices. In applications such as electronic or tactile skin in robotics, the stretchability can improve conformability with various curved parts [10].

The field of stretchable electronics has been widely reviewed in terms of materials and applications. For example, Bao *et al* reviewed the development of stretchable electronics in context with e-skin [17, 18]. Rogers *et al* focused on various materials and geometries for stretchable electronics [19–21]. Many other reviews have focused on different geometries and the role of materials is not much covered [22, 23]. Materials such as rubber-like nanocomposites have been extensively reviewed by researchers in terms of their electrical properties, synthesis and fabrication technologies [24, 25], but their role in stretchable electronics has not been reviewed yet. This review article bridges this gap and extends the discussion on nanocomposites towards stretchable electronics. Furthermore, we also discuss the correlation between the electrical and mechanical properties of the rubber-like nanocomposite, which were not discussed before. This article presents a detailed discussion on printable nanocomposites that can be used as stretchable interconnects.

In terms of historical perspective, the need and interest for the development of flexible electronics can be traced back to the 1960s, as shown in figure 1. The need to capture solar energy in space application and the energy crisis of late 1960s were the motivating factors for research on flexible electronics [26]. The shift from rigid to flexible solar panels was driven by the benefits of flexible panels such as a larger active area, lighter weight and more resistance to thermal and vibration shocks [26]. New applications such as flexible ribbons/wires in computers led to further growth in the use of flexible electronics. More recently,

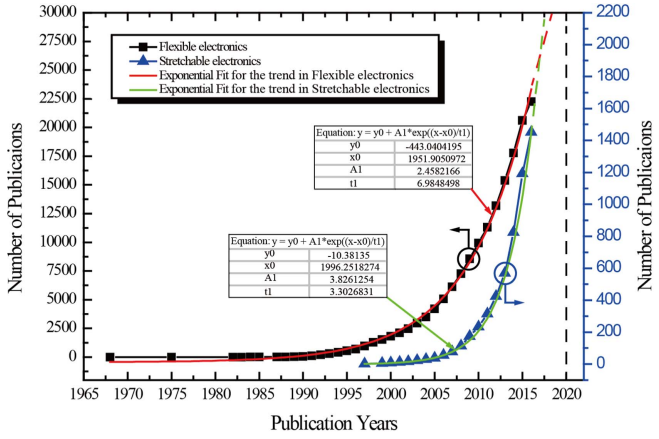

Figure 1. The trend from the accumulated number of publications during 1965 to 2020. The data was extracted from Web of science by searching keywords such as flexible electronics and stretchable electronics.

applications such as robotics and soft robotics [27], prosthetics [28], implantable electrodes [1], and wearable systems [29] etc, have led to significant growth in the field of flexible electronics. This is evident from the exponential increase in the number of publications in this field in last fifteen years (figure 1). By incorporating a degree of flexibility, the performance of multifunctional electronic systems could be extended for various applications. However, applications where large deformation is experienced, it is imperative to have stretchability. As an example, large deformation is experienced at complex surfaces such as the knees and elbows of a humanoid robot where the need for tactile skin has been highlighted by many researchers [10, 28, 30, 31]. However, flexible electronics with such large deformations and similar performance as traditional silicon-based electronics is not there yet. For this reason, the stretchability of tactile skin with rigid electronic components connected via stretchable interconnects has been explored as a solution in such cases. Likewise, stretchable electronics with islands of rigid electronic chips on flexible substrates and connected with each other via stretchable interconnects has been explored for wearable and biomedical applications [1, 32–34]. The stretchability also improves conformability of electronics with the body and thus improves the reliability of the measurement of vital health parameters via wearable systems. New materials such as graphene could add a new dimension to this research through features such as transparency and high electrical conductivity [35]. These advances have also led to the exponential growth in the field of stretchable electronics, especially in the past decade, as can be seen from figure 1. It can be noted that the growth in stretchable electronics is expected to surpass that in flexible electronics. This is perhaps due to the increasing number of applications requiring stretchable electronics. In terms of the actual number of publications, flexible and stretchable electronics are expected to attract about 15 000 and 5600 papers, respectively, by the year 2020.

This article is structured as follows: section 2 gives a general overview of stretchable interconnects and various structural geometries and materials are briefly discussed. Since these topics have been reviewed in past, the discussion of these topics has been intentionally kept brief and covered to serve the purpose of presenting a complete story. Section 3 describes different printing technologies to fabricate stretchable interconnects. Section 4 presents various materials for printable interconnects with a particular focus on the electrical and mechanical properties of nanocomposites. Then, several applications of stretchable interconnects, including those based on nanocomposites and various geometries are presented in section 5. Section 6 summarizes the review with key observations and future research directions.

2. A general overview of stretchable interconnects

Generally, stretchable systems can be obtained in two ways: (a) engineered shapes, and (b) rubber-like materials that are intrinsically stretchable. Figure 2 summaries various types of methods for stretchable interconnects from these two categories along with the maximum possible elongation achieved for each of them. Engineered geometries such as helical wires have been widely used for stretchable interconnects for a long time. The idea of helical conductive wire is straightforward; it resembles the structure of a spring or wire connecting a telephone receiver to its base in recent years [36, 37]. The helical shape makes the wire stretchable (rather expandable) and allows the telephone receiver to be moved away from the base. While telephone wires have vanished, thanks to the advent of wireless technology, the techniques of stretchable wires have found new applications, such as in a stretchable tactile skin. Expandable spiral electrodes,

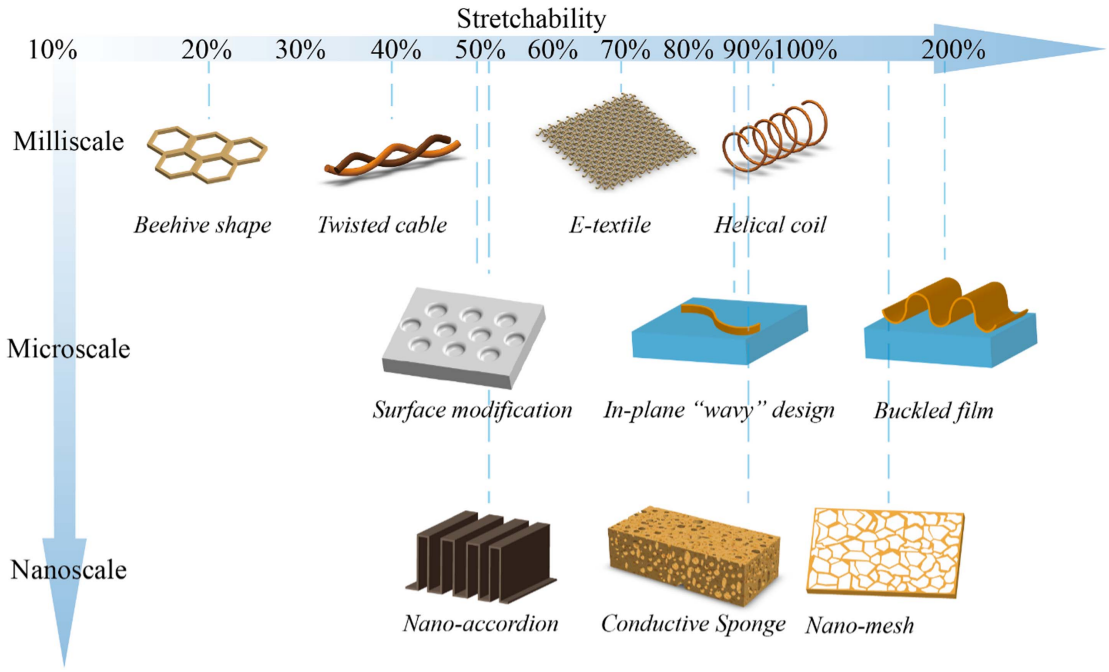

Figure 2. Various designs in engineered geometries of stretchable interconnect which are sorted according to their maximum elongations (stretchability) with respect to the scale of the structure size achieved by different patterning technologies.

obtained by winding the copper wires around an elastic nylon line, have been used to obtain large-area tactile skin [38]. Conductive thread-based clothing has been used in stretchable wearable electronics [39, 40]. Likewise, stretchable fabrics with knitted tactile sensing materials or tactile sensitive fabrics have been reported for stretchable tactile sensing [30, 41]. The fabrication of such stretchable systems often requires a core that can be chosen as the elastic thread. Then the conductive wire is wound around the core under a precise control in pitch and winding speed to build the helical shape. The wire can either be commercial copper wires [37] or elastic polymeric wires coated with highly conductive material (e.g. AgNW [36]). Depending on the winding pitch and wiring material, the failure strain of such designs can reach up to 100% with an increased resistance by 70% [36]. However, the large diameter of winding coil narrows the scalability of such geometries.

Another engineering technique for obtaining stretchable structures involves realizing conducting layers in 'wavy' or serpentine shapes [42–45]. Compared to the limited scalability possible in helical coil and threads, the geometry of in-plane 'wavy' design and buckled film can be easily scaled down to the microscale by microfabrication technology (figure 2). With a careful design of its 'wavy' amplitude, the curvature and the width, the optimized structure can be applied up to 90% strain with a negligible influence on electrical response [45]. The out-of-the-plane 'wavy' structure or the buckled film can either be deposited along with the buckled substrate [46] or partial-free standing on the substrate [11, 47]. The stretchability of wavy structures on buckled substrates mainly relies on the degree of pre-straining of the substrate which is limited due to the substrate's stretchability, on the other hand, the interconnects that are partial-free stand on the substrate can have a higher degree of stretchability benefit from the releasing from the substrate scheme. In this way, the stress generated at the interface between the conducting film and soft substrate can be avoided and this allows the film to have a longer possible elongation. Another strategy for stretchable conductors is to fabricate net-shaped conductive structures by releasing a pre-strained elastic substrate with conductive materials lying on it. Taking advantage of this technique, different stretchable conductors, such as metal-coated net films, wavy one-dimensional metal ribbons or two-dimensional metal membranes have also been demonstrated [48].

Stretchability of interconnects can also be enhanced by engineering the topography of the substrate. One such example is implementing mini-valleys on the surface of a soft substrate followed by metal coating. This results in a structure with a stable electrical behavior over a repeatable cyclic stretching [49]. Other than implementing mini-valleys on the surface of the substrate, the honeycomb lattice architecture or sponge-like structure is designed by introducing vias or air pores to the substrate. The conductive sponge can either be achieved by electrodeless-plating on commercially available PU sponge [50] or carbon nanotube sponge [51]. Recent research on multilayer graphene sponge has also generated much interest [52]. However, the idea of using conductive sponge for stretchable interconnects has several limitations including the size

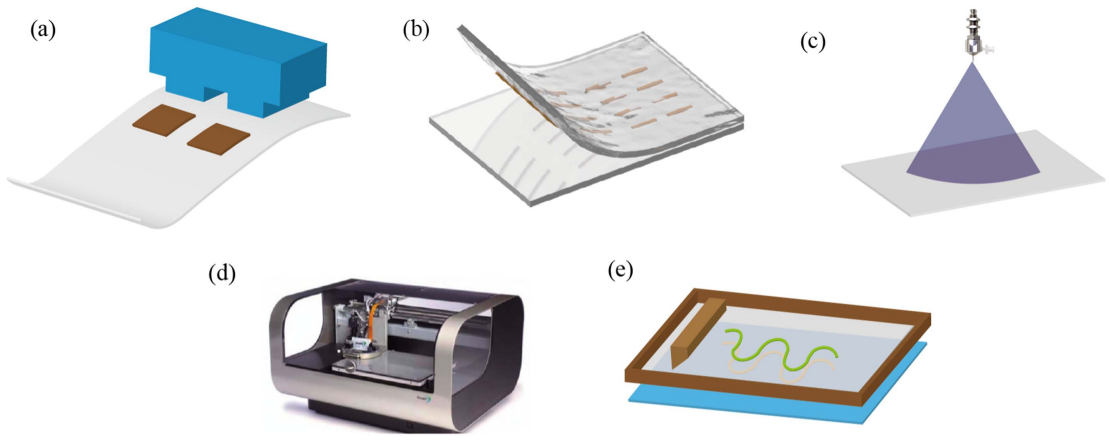

Figure 3. Printing technologies including (a) microcontact printing, (b) transfer printing, (c) spray coating, (d) inkjet printing, (e) screen printing.

of pores in the sponge, which decides both the minimum dimension of the interconnects and the stretchability of the interconnects. With smaller pore size the interconnect structure could be finer, but at the same time less stretchable. Further, there are challenges related to the integration and soldering of such structures as the pores in the structure do not allow seamless integration as in conventional electronics. Some technologies can realize a very fine structure of interconnects. For example, the nano-mesh structure fabricated by grain boundary lithography. This nanoscale structure can withstand strain up to 160%. However, after 1000 cycles' test, the resistance changed significantly [53]. Another example is the nano-accordion structure, which is made of Al doped ZnO. This structure can be elongated up to around 53%, but in the meantime the resistance changed dramatically [54].

A truly stretchable conductor should be like rubber—stretching and regaining the original shape after release, and ideally with negligible variation in the conductivity. Such interconnects are discussed in details in the following sections of this review. Few examples of this type of (non-ideal) stretchable conductor include elastic conductors based on Single-Walled Carbon Nano Tubes (SWNT)-PDMS composite films embedded in PDMS or coated with dimethylsiloxane-based rubber [55–58]. In these interconnects, the nanotubes carry the electricity and the rubber provides the stretchability. These conductors allow uniaxial and biaxial stretching of 70%–100%—without mechanical or electrical damage. The microfluidics approach is yet another interesting alternative that has been developed in recent years to obtain stretchable conductors. In this approach, the wires are replaced with conductive liquid confined in microfluidic channels [59]. These approaches are not yet at a stage where they can be employed in large area integration. Nonetheless, recent advances in material engineering, highlighted in this article, do raise hope.

3. Technologies for printed stretchable interconnects

Printing technologies are widely used for the development of flexible and stretchable electronics as they offer a cost-effective fabrication alternative to lithography-based approaches [60]. As illustrated in figure 3, these technologies encompass a number of methods including microcontact printing, transfer printing, spray coating, inkjet printing and screen printing [60]. An excellent overview of various printing technologies for flexible electronics is given in [60]. The technologies most relevant to stretchable interconnects are briefly described here. These printing techniques are preferred over other patterning techniques such as photolithography and electron beam lithography for the development of large area electronics applications owing to their low cost and fast processing speed, which make them attractive in terms of manufacturing [60]. The materials, which are compatible with printing technologies, range from conductors, dielectrics, and semiconductors in the form of dispersed solution, colloids and paste. The concept of printing technology is to spread and pattern the ink/paste directly on the substrate with the help of specific printing equipment. For instance, microcontact printing involves a prefabricated stamp gaining contact with the conductive ink first and this is followed by contact with the target substrate under specific pressure, as described in figure 3(a). The reported resolution can reach a line width of 314 μm with a space of 286 μm [61]. The stamp in the process can be repeatably used. However, with an overload contact pressure the stamp can easily pick up excessive ink, which affects the final resolution of the printed structures. More precise patterns with a minimum structure of up to 5 μm resolution can be achieved with the help of a Nanoimprint machine [62]. Another popular printing technology is spray coating (figure 3(c)). This technology utilizes a nozzle to spray solution-based materials on the substrate.

Spray coating has the advantage of efficient material usage but the resolution can be poor. It is often used in combination with other printing technologies such as contact printing or transfer printing [63–66]. Compared to spray coating, inkjet printing can realize a versatile pattern directly from graphical designs (figure 3(d)). The achievable resolution by spray and inkjet printing is hugely dependent on parameters such as the diameter of the nozzle and the distance between the targeting substrate, etc [67, 68]. The limitation of the nozzle diameter restricts the size of the particle in the ink used for these printing technologies. In this regard, solution-based or colloid-based ink is preferred for homogeneous coating and the relevant printing technologies are called screen or stencil printing. Screen printing utilizes a paste-like ink which is more viscous compared to spray and inkjet printing. As shown in figure 3(e), the setup of screen printing comprises of a stencil, squeegee, a press bed and the substrate, The resolution is limited by the mesh size from the stencil, the viscosity of the ink, the surface energy of the substrate and the speed of printing etc [69, 70]. The viscosity of the ink has to be carefully controlled to avoid the over-spreading of printed ink and to control the printing resolution. Currently, the highest resolution of this technology is about 50 μm [71].

4. Materials for printed stretchable interconnects

4.1. Intrinsic conductive and elastic interconnects

Traditionally, metals such as gold and copper have been preferred for interconnects and electrodes, owing to their high electrical and thermal conductivity that permits an influx of large current and fast transmission of signals. However, when it comes to stretchability the metals have been found to have limited use as they are not elastic enough [46, 72]. For example, the metal interconnects exhibit an elastic modulus of about 100 GPa. On the other hand, highly stretchable elastomers such as PDMS and PU etc, which are often used as highly stretchable substrates, exhibit an elastic modulus below 1 MPa. For this reason, the use of metal for a stretchable interconnect application has been achieved through engineered geometries described in section 2. The stretchable interconnects that act like rubber, i.e. stretching and regaining the original shape after release, with negligible variation in the conductivity, offer an interesting alternative. These interconnects are based on various nanocomposites, which are made by mixing a variety of conducting filler materials in a matrix of soft and rubbery materials. A comparison of the elastic modulus and electrical conductivity of various insulating polymers, metal and carbon-based filler materials is given in figure 4. While mechanical stretchability and electrical conductivity are prerequisites for stretchable interconnects, the interaction between the conductor and polymer substrate is crucial as well. Huge differences in elastic modulus between the substrate and conducting materials can lead to a highly concentrated stress at the interface and thus can have unreliable operation [46]. In order to mitigate this effect, novel conductive materials that can balance the mechanical stretchability and electrical conductivity are in high demand. A few examples of intrinsic conductive and stretchable materials are presented in figure 5.

Organic conductive polymers have emerged as popular candidates for filler materials, owing to their acceptable electrical conductivity and mechanical softness [6]. Some of the widely used organic conductors include Polyaniline (PANi) [73] and Poly(3, 4-ethylenedioxythiophene): poly(4-styrenesulfonate) (PEDOT:PSS) [74]. They have modest electrical conductivity (~100 S cm^{-1}) and are soft enough for up to 10% stretching without any cracks in the film [74]. Furthermore, being transparent they can be used in optoelectronic device applications [75, 76]. The electrical conductivity of these conductive polymers is limited. In the case of PEDOT:PSS, the highly conductive PEDOT grains are surrounded by excess weakly ionic-conducting PSS. Although the PSS ions help PEDOT to be easily dispersed in water, it separates PEDOT from establishing a conductive path [77]. A secondary doping can improve the electrical conductivity of the resulting PEDOT:PSS film [75, 78] and the maximum conductivity can be in the order of 1000 S cm^{-1}, which is still low in comparison with metals. An example of PEDOT:PSS, replacing ITO in solar cells is given in figure 5(a) [79].

Another type of filler material is the ionic-Hydrogel electrode, which is made of PAM-Aam (LiCl) and is highly elastic and electrically conductive [80]. The elastic modulus of ionic-hydrogel electrode filler material is lower than an elastomeric substrate such as Ecoflex. Therefore, the substrates deposited with ionic-hydrogel electrode do not show any phenomenon of delamination even when they are stretched up to 500%. Besides conductive polymers, liquid metals such as eutectic gallium-indium (EGaIn) incorporated within microchannels in an elastic polymeric substrate [81] are also investigated for stretchable interconnect applications. The use of EGaIn as stretchable interconnects to connect LEDs is shown in figure 5(b) [82]. Although they result in a reliable and robust interconnect system, the complexity associated with fabrication and encapsulation of microchannels in such structure limits their use. Another popular group of materials for stretchable interconnects is the conductive nanocomposite. These nanocomposites have highly conductive fillers dispersed within the elastic polymer matrix and their electrical conductivity can be tuned by varying the load volume of the filler material. The achieved electrical conductivity can reach up to the level of 10^6 S m^{-1} and the stretchability can be up to 100% [83]. A few examples of screen printed

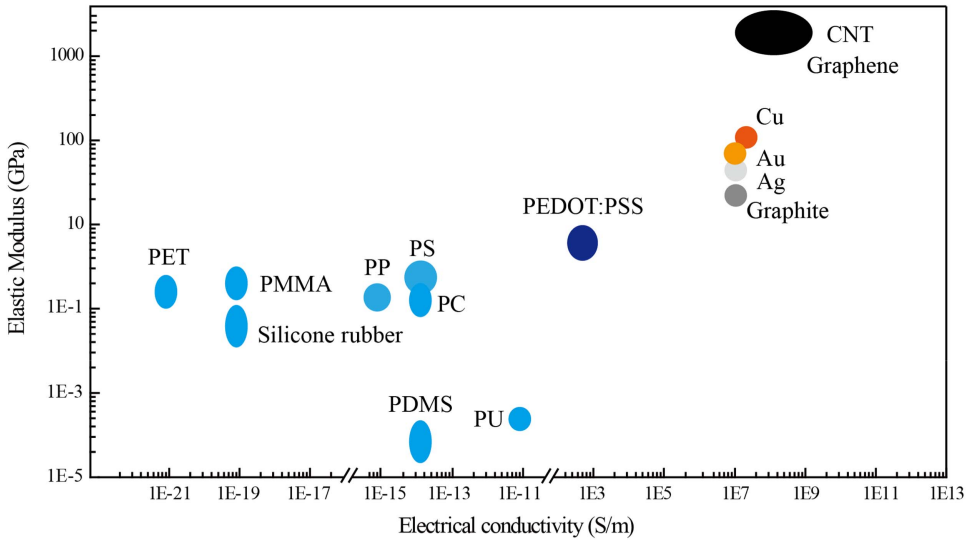

Figure 4. Comparison of the elastic property of various materials (including insulating polymers, organic conductive polymer, metals and carbon materials) for stretchable interconnects with electrical conductivity.

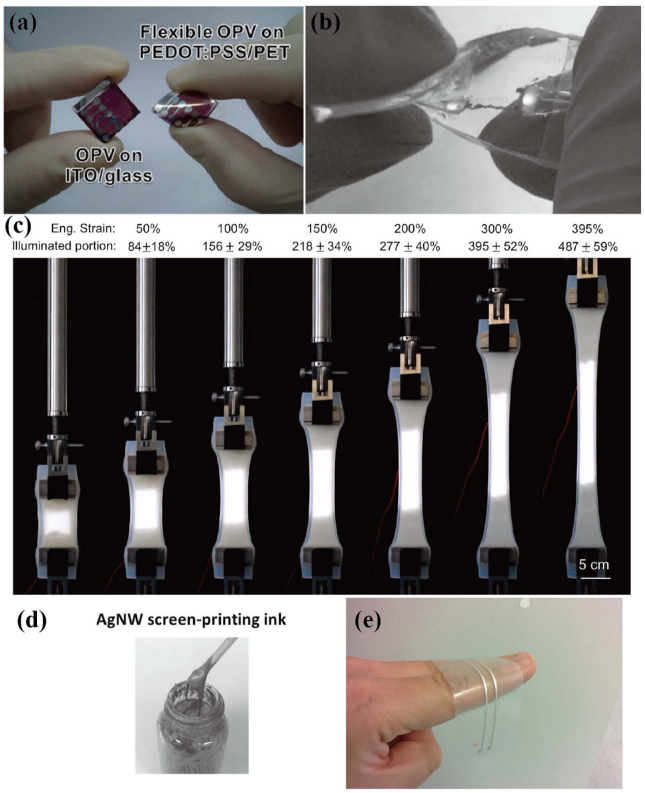

Figure 5. (a) Flexible OPV based on PEDOT:PSS. Reprinted from [79], copyright 2011, with permission from Elsevier. (b) Liquid metal interconnected LED, [82] John Wiley & Sons. © 2013 WILEY-VCH Verlag GmbH & Co. KGaA, Weinheim. (c) Ionic Hydrogel-based stretchable electrode. From [80]. Reprinted with permission from AAAS. (d) Commercially available AgNW-based screen-print ink, [71] John Wiley & Sons. © 2016 WILEY-VCH Verlag GmbH & Co. KGaA, Weinheim. (e) Stretchable interconnects based on screen-printed silver paste. Reproduced from [84]. CC BY 4.0.

nanocomposites for stretchable interconnects are shown in figures 5(d)–(e) [71, 84]. The conductive nanocomposites show strong advantages over the organic polymer, ionic hydrogel and the liquid metal in terms of electrical conductivity and mechanical elasticity. This article is focused on a composite based on a variety of conductive fillers which is composed of metal-based fillers, carbon-based fillers and semi-conductor-based fillers. A detailed study of these materials is presented in the following section.

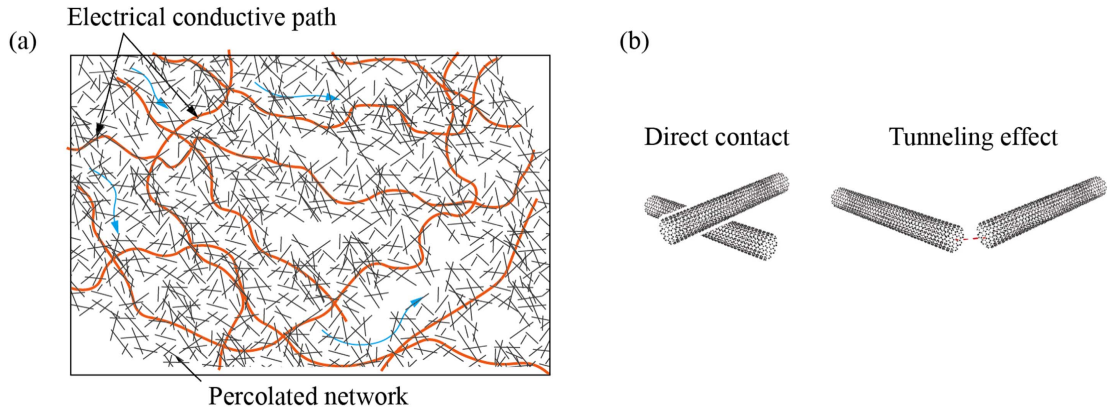

Figure 6. Schematic diagram of the theory of a percolated network and tunneling effect between adjacent nanowires.

4.2. Nanocomposite-based stretchable electrode

Conductive nanocomposites benefit from the high electrical performance of fillers dispersed in the elastic polymer matrix. The synthesis of these nanocomposites with an appropriate mix of fillers in the polymer matrix is critical in terms of performance. The synthesis process requires three following essential elements: the conductive filler, the binder (polymer matrix) and the solvent [71]. To make sure the fillers are homogeneously dispersed in the matrix, an appropriate solvent is selected to de-bundle the fillers. Simultaneously, the sonication power and duration should be tuned to transduce the energy for dispersing the filler homogenously without breaking them [85]. In general, the electrical behavior will be enhanced if the loading ratio of fillers is increased. However, the elastic modulus of the resulting composite is also increased in the process and therefore a trade-off is needed between the elastic modulus and electrical conductivity. The following sub-sections describe the theory governing this trade-off and a comparison of various nanocomposites based on a variety of conductive fillers.

4.2.1. Percolation and tunneling theory

The conductivity of nanocomposites varies as a result of the variations in filler concentration [10]. The conductivity is governed by the percolation theory, which is represented by [60, 86]:

$$\sigma \approx \sigma_0 (p - p_c)^t, \quad \text{for } p > p_c \tag{1}$$

Where σ is the bulk conductivity of the composite, σ_0 is the conductivity of the filler, p weight percentage of the filler and t the critical exponent. The critical percentage p_c of the filler is defined as the percolation threshold. This critical fraction is achieved when a continuous electrical path is built, as illustrated in figure 6 [86]. Several parameters affect the value of the percolation threshold and these include the dimension of filler, morphology of the filler, and the synthesis method of the nanocomposite. Many numerical simulation and mathematical modelling studies have been done to investigate the effect of the filler's dimension on the percolation threshold of the nanocomposite [87–89]. In Balberg *et al*'s theory, a denser composite system can be modelled as a lattice-like system and its percolation threshold is strongly dependent on the density and dimension of the fillers [90]. Some researchers have performed studies based on a Monte Carlo simulation that regards a percolated network as a statistic problem. Both studies suggest that the percolated threshold is proportional to the reciprocal of the particle's aspect ratio [91] and can be mathematically written as:

$$p_c \propto \frac{1}{r}, \quad r = \frac{L}{D} \tag{2}$$

The experimental results obtained from various nanocomposites and plotted in figures 7(b) and (c) are in line with the above theoretical relationship between the percolation threshold and the aspect ratio. Extending this relationship further, figure 7(a) also shows the correlation between the maximum conductivity and aspect ratio of fillers among various nanocomposites. The global conductivity of the percolated network within the polymer matrix depends on the conductivity of the filler, the contact resistance between the overlapped fillers and conductivity of the electron tunnelling effect through the nearby fillers [92]. The distance of the tunnelling effect d_{tunnel}. can be estimated as:

$$d_{\text{tunnel}} = \hbar / \sqrt{8 m_e \Delta E} \tag{3}$$

Where, $\hbar$ is the Planck's constant, m_e is the mass of electron and ΔE is the difference in work function between filler and polymer matrix. However, this tunnelling effect can be ignored if the wrapped polymer between adjacent nanowires is thicker than a cutoff distance d_{cutoff} [92].

4.2.2. Elastic modulus of composite materials

The studies estimating the elastic modulus of composite materials can date back to the 1970s [93]. The general form for the elastic modulus of a nanocomposite is described as [94]:

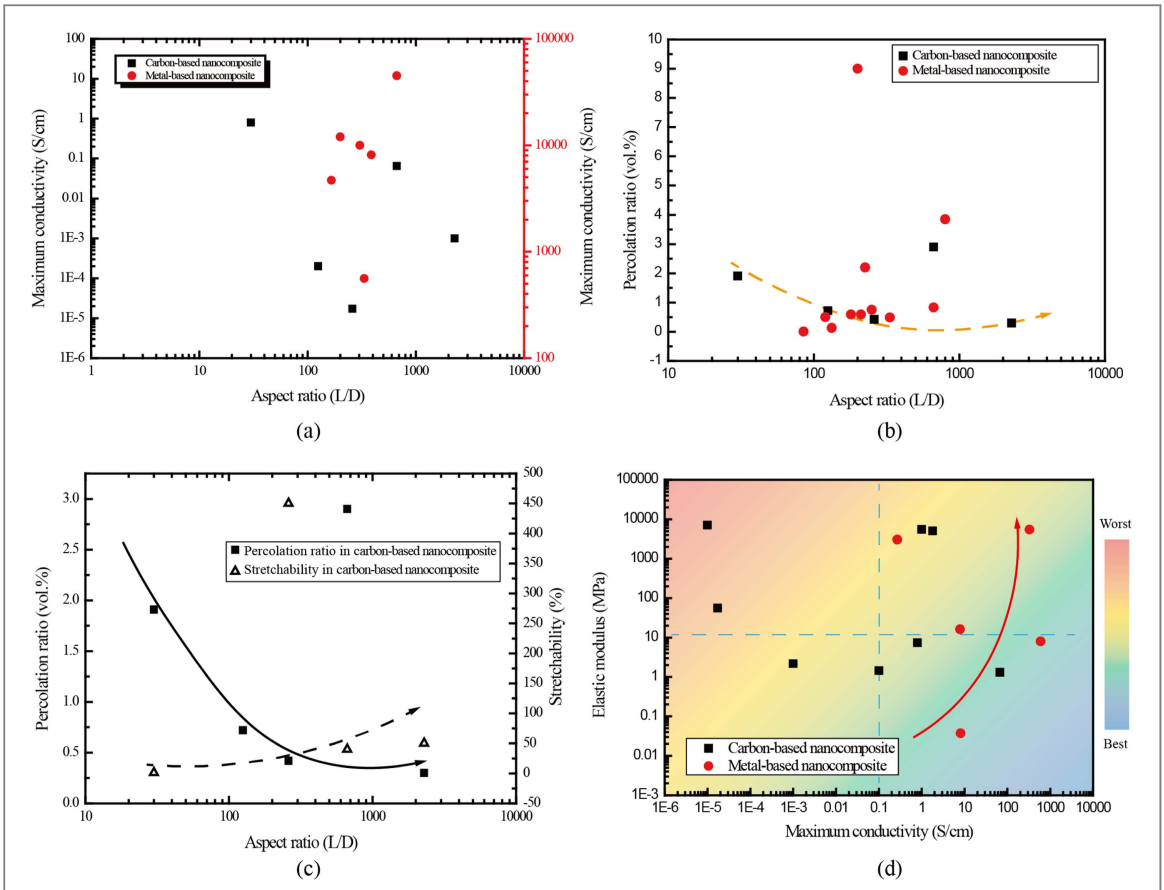

Figure 7. Plot of data points collected from tables 1 and 2. (a) Correlation between the maximum conductivity and aspect ratio of fillers from various nanocomposites. (b) Correlation between the percolation ratio and aspect ratio among various nanocomposites. (c) The trend of the percolation ratio and stretchability with respect to the aspect ratio for carbon-based nanocomposites. (d) The mapping of data points with the elastic modulus against the maximum conductivity.

$$\frac{M}{M_1} = \frac{1 + AB\phi}{1 - B\phi} \text{ where } B = \frac{M_2 / M_1 - 1}{M_2 / M_1 + A} \quad (4)$$

Where M represents the elastic modulus of composite and M_1 and M_2 are the modulus of polymer matrix and filler respectively. ϕ is the volume fraction of fillers and A is a critical parameter defined by the geometry of filler and the Poisson's ratio of polymer matrix. This general equation skips some factors such as the sediments and aggregations of fillers, but it gives a fair estimation of the mechanical property of the resulting composite.

4.2.3. Carbon-based nanocomposite

Carbon particles are often used as conductive fillers because they are widely available, have high electrical conductivity and low cost. Many studies on carbon-based composites in stretchable interconnects are listed in table 1. It can be noted that graphite is one of the most widely used carbon fillers for stretchable and conformable electrodes. In order to achieve the desired level of electrical conductivity a large amount of fillers are used, which also leads to the degradation of stretchability in graphite-based composites [95]. On the other hand, owing the high aspect ratio of CNTs, the conductivity of CNT-based nanocomposites can be higher with a much lower percolation threshold [96]. However, due to the strong Van der Waal forces among carbon fillers, they tend to bundle and entangle together which leads to an inhomogeneous conductivity and high load ratio. By evaluating the maximum conductivity of various nanocomposites, it is observed that the group of Graphene Nanoplatelets nanocomposites exhibit superior conductivity with a low percolation ratio. This is because graphene has large surface area of 2630 m^2g^{-1} and high electrical conductivity 7200 $s \cdot m^{-1}$ [97].

4.2.4. Metal-based nanocomposites

Metal-based composites generally comprise of metallic nanoparticles or nanowire (NWs) as filler materials. They are popular owing to their higher conductivity compared to carbon-based fillers. Silver flakes are often found in commercially available conductive inks. Recently, stretchable and conductive silver-based inks have been commercialized as well [84]. The reported silver ink shows a high conductivity in the range of 10^3–10^4 S cm^{-1}, as shown in table 2. The high aspect ratio AgNW further enhances the electrical conductivity. However, the maximum conductivity of the AgNW nanocomposite does not indicate a strong correlation with the aspect ratio of NWs. In general, the percolation ratio of AgNW nanocomposites is low.

Table 1. Comparison of various nanocomposites based on carbon fillers with respect to properties such as filler size, percolation ratio, maximum conductivity and mechanical elasticity.

Material (Filler-polymer matrix)	Filler size	Aspect ratio (L/D)	Percolation ratio	Maximum conductivity	Elastic Modulus	Elongation	Reference
Graphite-PDMS	25.4 μm	—	11.1 vol.%	1.8 S cm^{-1}	5.1 GPa	0.71%	[95]
Graphite-PDMS	10 μm	—	12 vol.%	2 × 10^{-6} S cm^{-1}	—	—	[98]
Graphite-Epoxy	D: 10 μm, t: 0.1 μm	—	1.3 vol.%	1 S cm^{-1}	5.56 GPa	—	[99]
Graphite-PU[a]	D: 10 μm, t: 0.1 μm	—	1.7 vol.%	1 × 10^{-5} S cm^{-1}	7.14 GPa	—	[99]
Graphite-Epoxy	4–44 μm	—	20 vol.%	3.3 × 10^{-2} S cm^{-1}	—	—	[100]
Graphite-Phenolic Resin	< 1 μm	—	15 vol.%	66.7 S cm^{-1}	1.3 MPa	—	[101]
Graphite-PP[b]	21.3 μm	—	—	20.16 S cm^{-1}	—	—	[102]
Graphite-PVDF[c]	21.3 μm	—	—	0.56 S cm^{-1}	—	—	[102]
Graphite-LDPE[d]	2.1–82.6 μm	—	2.1 μm → 13.5 vol.% 82.6 μm → 25.5 vol.%	1 S cm^{-1}	—	—	[103]
[e]EG-PANI	L: 400 nm, t: 10–40 nm	—	0.91 vol.%	35 S cm^{-1}	—	—	[104]
[f]GNP- PE[g]	L: 39–115 nm t: 3.6–7.1 nm	—	0.51, 1.2, 2.4 vol.%	—	—	—	[105]
[h]G-ODA-PDMS	t: 2.7 nm	—	0.63 vol.%	2 × 10^{-6} S cm^{-1}	—	—	[97]
Graphite-PS[i]	D: 6.5 μm, t: 100–300 nm	—	3.5 vol.%	1 × 10^{-5} S cm^{-1}	—	—	[106]
[j]MWCNT-PDMS	L: 1–25 μm	—	2.1 vol.%	0.1 S cm^{-1}	1.43 MPa	45%	[96
MWCNT-PDMS	L: 5–15 μm D: 60–100 nm	125	0.72 vol.%	2 × 10^{-4} S cm^{-1}	—	—	[107]
MWCNT-PDMS	L: 30–50 μm D: 15–20 nm	2285	0.3 vol.%	1 × 10^{-3} S cm^{-1}	2.18 MPa	50%	[108]
MWCNT-PDMS	L: 10–30 μm D: 20–40 nm	666	2.9 vol.%	6.5 × 10^{-2} S cm^{-1}	—	40%	[61]
MWCNT-PDMS	L: 1–2 μm D: 40–60 nm	30	1.91 vol.%	0.8 S cm^{-1}	7.38 MPa	1.2%	[109]
[k]CNF-PU	L: 30 μm D: 80–150 nm	260	0.42 vol.%	1.72 × 10^{-5} S cm^{-1}	56 MPa	450%	[110]

[a] PU: Polyurethanes,
[b] PP: Polypropylene,
[c] PVDF: Poly(vinylidene fluoride),
[d] LDPE: Low density polyethylene,
[e] EG: Exfoliated graphite,
[f] GNP: Graphene Nanoplatelets,
[g] PE: Polyethylene,
[h] G-ODA: Alkyl-functionalized graphene,
[i] PS: Polyester,
[j] MWCNT: Multi-walled carbon nanotube,
[k] CNF: Carbon Nanofiber.

With a minimum ratio of 0.005 vol.%, their conductivity can reach 2.3×10^{-2} S cm^{-1} [111]. On average, the stretchability of AgNW nanocomposites can reach 115%, which makes AgNW nanocomposites good candidates for stretchable interconnects. Some other metallic NW-based composites show a similar performance to AgNWs. Although metal-NWs have the advantages of higher conductivity with a lower elastic modulus suitable for stretchable interconnects, they are not free from challenges. For example, since metallic NWs are manufactured in a solution-based method the insulating ligands in the solvent should be removed to obtain a low contact resistance between adjacent NWs. Usually, a post-treatment process such as thermal annealing is introduced for this purpose and this poses a challenge for devices on polymeric substrates. The idea of introducing a conductive polymer PEDOT:PSS to realize the nano-soldering process among wires dramatically improves the performance of interconnects [112]. Other solutions, such as a hybrid system with AgNWs and other materials (CNTs [113] and Graphene [114]) also show a highly stretchable and conductive performance.

4.3. Discussion4.3.1.

Studying the data from tables 1 and 2, the correlation among many factors such as material type, aspect ratio of fillers, percolation ratio, and elastic modulus in the nanocomposite can be established. As shown in figure 7(a), even with a similar aspect ratio of the filler, the maximum achieved conductivity of a metal-based nanocomposite is several orders higher than a carbon-based nanocomposite. This is due to the high electrical conductivity of metal. From the plots, it is clear that the maximum conductivity does not show any reliance on the filler's aspect ratio. However, the aspect ratio has a strong effect on the percolation ratio as shown in figure 7. Viewed from the data illustrated in figure 7(b), the four data points from the carbon-based nanocomposite are all composed of MWCNTs with PDMS and this excludes the influence of material property. The trend, indicated in dashed line, shows a reciprocal relation between the aspect ratio of the filler and the percolation ratio, which matches with theoretical relationship in equation (2). In contrast, the metal-nanocomposites do not reveal any such trend. Within a large range of aspect ratio of metal fillers (100–1000), nanocomposites have a low percolation ratio (<1 vol.%). This could be attributed to the fact that the metal fillers, as compared to the carbon fillers, do not get entangled due to their straightness and passive oxide structure. The SEM images in figure 8 compare the CNT with metal NWs. It can be seen the CNT has a tortuous morphology while the AgNWs are straight. The influence of the filler's aspect ratio is not only reflected in a reduced percolation ratio, but also in the improved stretchability. If the parameter of stretchability is added into the diagram between the aspect ratio and percolation ratio of the carbon-based nanocomposite (figure 7(c)), it is clear that the high aspect ratio of the fillers gives higher stretchability. In practice, there is always a trade-off. The higher the ratio of fillers, the higher the conductivity of the nanocomposite, and the lower the elastic property. According to the collection of data points presented in figure 7(d), most points of carbon-based nanocomposites lie below the conductivity of 1 S cm^{-1} with a large difference in the elastic modulus. In contrast, a trend indicated by the red arrow line can be found in metal-based nanocomposites, of which the higher conductivity leads to a higher elastic modulus. Still, a point with high conductivity (~10 S cm^{-1}) and low elastic modulus (~40 kPa) can be found. The blue highlighted area indicates the region suitable for stretchable interconnects while the red area is the direction that should to be avoided.

5. Application

A wide range of applications requiring stretchable interconnects are shown in figure 9. In these applications, only flexibility of the electronic system is insufficient to meet the requirements as they experience large deformations during bending. The development of stretchable interconnects to integrate multifunctional sensors and electronics has filled this gap and in fact the field has grown exponentially in line with the trend presented in figure 1. Figure 9(a) shows the serpentine-shaped stretchable interconnects realized with a MWCNT-PDMS nanocomposite. Figure 9(b) demonstrates a smart prosthetic hand equipped with artificial skin that is able to detect various signals such as humidity, temperature, pressure, etc [137]. Some applications of stretchable electronics can make a huge difference and accelerate the progress of medical treatment. For example, the balloon catheter often used in surgery to eliminate blood blockage requires up to 130% stretching when inflated. Stretchable interconnects on such a balloon catheter with pressure sensors is illustrated in figure 9(c). The stretchable interconnects enable the overall electronic system to withstand large deformation while giving electrical feedback to surgeons in order to help improve the performance of surgery [1]. Other clinically relevant information like temperature can be monitored from human skin *in situ* (figure 9(d)) [138]. In this case, a 24 h or even longer time thermometry data can be collected by the surgeon or clinician, which can improve medical treatments. For applications where more precise surgeries and signal monitoring are required, stretchable neural electrodes [33] have been developed. Applications in wearable electronics for motion detection (figure 9(e)) have also benefited from stretchable electronics. These applications have integrated electronics to wearable cloths such as bandages and gloves [139]. Not only have stretchable mechanical sensors have been developed, stretchable chemical sensors have also shown promising

Table 2. Comparison of various nanocomposites based on metal fillers in terms of properties such as filler geometry, percolation ratio, maximum conductivity and mechanical elasticity.

Material (filler-polymer matrix)	Filler size	Aspect ratio (L/D)	Percolation ratio	Maximum conductivity	Elastic Modulus	Elongation	Reference
Ag flakes-PU	2–3 μm	—	56 vol.%	3.6×10^3 S cm^{-1}	—	600%	[115]
AgNW-poly(acrylate)	L: 5–15 μm D: 60 nm	83–250	—	7.84 S cm^{-1}	16.25 MPa	50%	[116]
Ag Powder-PDMS	2–3.5 μm	—	12.6 vol. %	6×10^2 S cm^{-1}	8 MPa	150%	[117]
AgNW-PUA[a]	L: 15–25 μm D: 25–35 nm	666	0.83 vol.%	4.5×10^4 S cm^{-1}	—	70%	[71]
AgNW-PDMS	L: 20–50 μm D: 115 nm	304	—	9.97×10^3 S cm^{-1}	—	100%	[118]
AgNW-PDMS	L: 10–60 μm D: 90 nm	388	—	8.13×10^3 S cm^{-1}	—	15%	[119]
Ag flakes-PU	—	—	—	4.31×10^4 S cm^{-1}	—	74%	[84]
AgNW-PDMS	L: 10 μm D: 60 nm	166	—	4.69×10^3 S cm^{-1}	—	150%	[120]
AgNW-PDMS	L: 10–60 μm D: 90 nm	388	—	8.13×10^3 S cm^{-1}	—	80%	[121]
AgNW-PDMS	L: 80 μm D: 100 nm	800	3.85 vol.%	20 S cm^{-1}	—	35%	[122]
AgNW-poly(TBA-co-AA)[b]	L: 20 μm D: 60 nm	333	—	5.6×10^2 S cm^{-1}	—	160%	[123]
AgNW-PLA[c]	L: 8 μm D: 60 nm	133	0.13 vol.%	0.27 S cm^{-1}	3048 MPa	3%	[124]
AgNW-MC[d]	—	—	0.29 vol.%	3.3×10^2 S cm^{-1}	5519.9 MPa	—	[125]
AgNW-PEDOT:PSS	L: 10–30 μm D: 90 nm	222	2.5% Areal fraction	10^4 S cm^{-1}	—	—	[126]
AgNW-PEDOT:PSS	L: 50–100 μm D: 10 nm	7500	—	0.73×10^3 S cm^{-1}	—	120%	[127]
AgNW-PEKK[e]	L: 10–100 μm D: 120–400 nm	211	0.59 vol.%	1 S cm^{-1}	—	—	[128]
AgNW-PC[f]	L: 10 μm D: 117 nm	85	0.005 vol.%	2.3×10^{-2} S cm^{-1}	—	—	[111]
AgNW-PA11[g]	L: 30–60 μm D: 200–300 nm	180	0.59 vol.%	2.7 S cm^{-1}	—	—	[129]
AgNW-PS	L: 10–60 μm D: 70–140 nm	333	0.489 vol.%	10 S cm^{-1}	—	—	[130]
AgNW-SBS[h]	L: 30 μm	200	9 vol.%	1.2×10^4 S cm^{-1}	—	100%	[83]

Table 2. (Continued.)

Material (filler-polymer matrix)	Filler size	Aspect ratio (L/D)	Percolation ratio	Maximum conductivity	Elastic Modulus	Elongation	Reference
CuNW-PVA[i]-PDMS	D: 150 nm L: 20 μm D: 60 nm	333	—	8.1 S cm^{-1}	37.5 kPa	60%	[131]
CuNW-GFRHybrimer[j]	L: 35 μm D: 50 nm	700	—	4.8 S cm^{-1}	—	—	[132]
CuNW-PS	L: 3 μm D: 25 nm	120	0.25–0.75 vol.%	10^{-6} S cm^{-1}	—	—	[133]
CuZr-PDMS	—	—	—	1.32×10^{4} S cm^{-1}	—	70%	[134]
NiNW-P(VDF-TrFE)[k]	L: 50 μm D: 200 nm	250	0.75 vol.%	1 S cm^{-1}	—	—	[135]
AuNW-P(VDF-TrFE)	L: 45 μm D: 200 nm	225	2.2 vol.%	1 S cm^{-1}	—	—	[136]

[a] PUA: Polyurethane acrylate,
[b] Poly(TBA-co-AA): Poly(tert-butylacrylate-co-acrylic acid),
[c] PLA: Polylactide,
[d] MC: Methylcellulose,
[e] PEKK: Poly(ether ketone ketone),
[f] PC: Polycarbonate,
[g] PA11: Polyamide 11,
[h] SBS: Styrene butadiene styrene,
[i] PVA: Poly(vinyl alcohol),
[j] GFRHybrimer: Glass-fabric reinforced plastic film,
[k] P(VDF-TrFE): Poly(vinylidene difluoride)- trifluoroethylene.

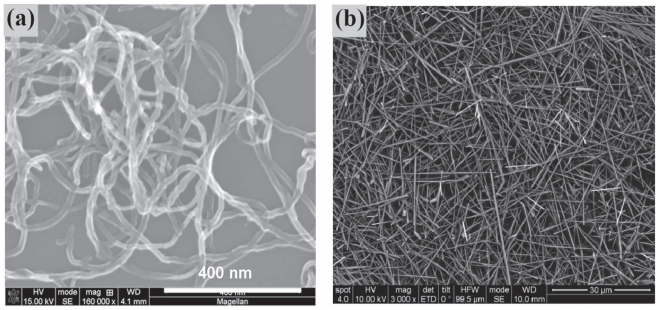

Figure 8. SEM images of (a) a carbon nanotube. Reprinted from [144], copyright 2013, with permission from Elsevier. (b) AgNWs. Reproduced from [145]. © IOP Publishing Ltd. All rights reserved.

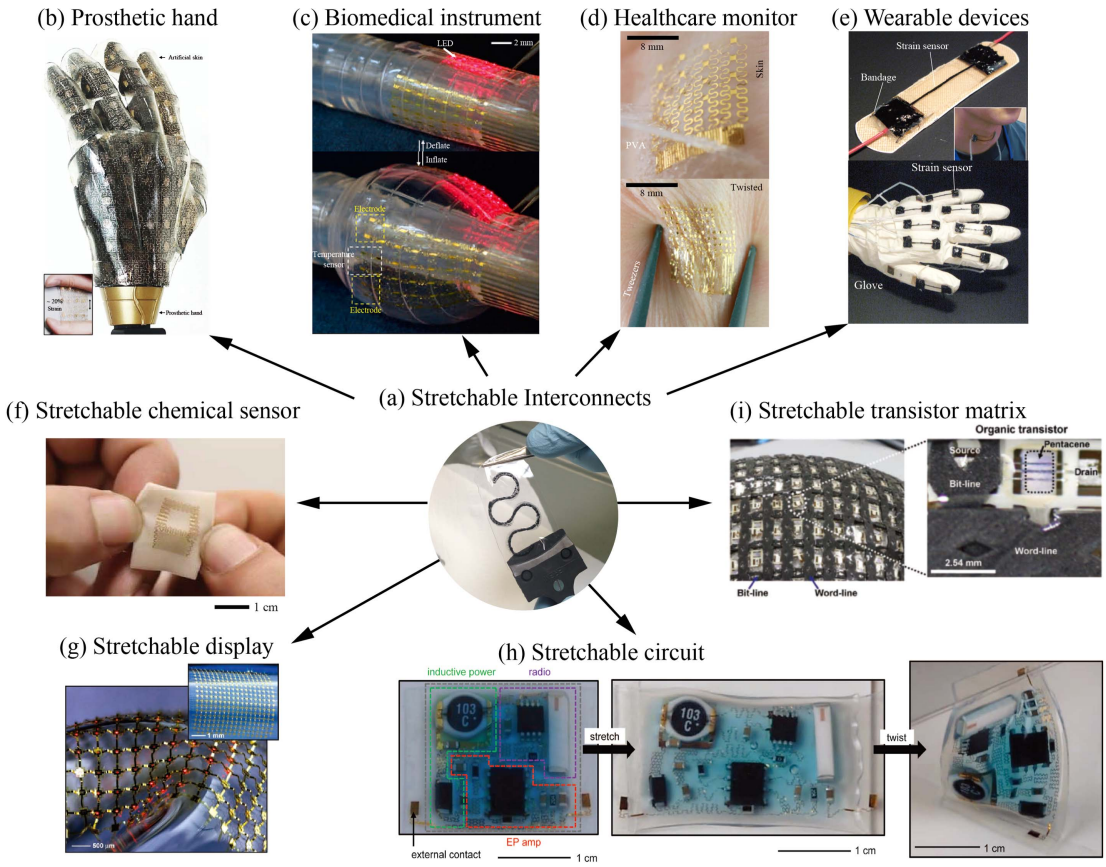

Figure 9. (a) Stretchable interconnects based on a MWCNT-PDMS nanocomposite. (b) Artificial skin for a prosthetic hand. Reprinted by permission from Macmillan Publishers Ltd: Nature Communications [137], copyright 2014. (c) Balloon catheter integrated with electrodes and temperature sensors. Reprinted by permission from Macmillan Publishers Ltd: Nature Materials [1], copyright 2011. (d) Thermal monitoring sensor system for human skin. Reprinted by permission from Macmillan Publishers Ltd: Nature Materials [138], copyright 2013. (e) Strain sensor integrated with a bandage and glove. Reprinted by permission from Macmillan Publishers Ltd: Nature Nanotechnology [139], copyright 2011. (f) Stretchable chemical sensor for sweat detection [141] John Wiley & Sons. © 2014 WILEY-VCH Verlag GmbH & Co. KGaA, Weinheim. (g) Stretchable display based on an inorganic LED. From [142]. Reprinted with permission from AAAS. (h) Stretchable circuits for EEG signal detection and transmission. From [143]. Reprinted with permission from AAAS; and (i) a stretchable transistor matrix. From [55]. Reprinted with permission from AAAS.

results. The complete stretchable device shown in figure 9(f) is able to give an epidermal analysis of biofluids like sweat and is able to undergo stretching [140, 141]. Regarding consumer electronic applications, stretchable displays have been developed by interconnecting rigid inorganic light emitting diodes (ILED) with non-coplanar stretchable interconnects [142]. For a multi-functional wearable system, the serpentine-shaped stretchable interconnects allow rigid electronic components including signal detection electrodes, inductive power, amplifier and data transmission coil to form a stretchable network as shown in figure 9(h). Such networks enable an efficient method of data collection. Even weak electrophysiological signals can be detected and transmitted. Furthermore, this network is robust against any stretching and twisting movement [143].

Interconnects to form a stretchable circuit can be realized by intrinsic conductive and stretchable materials as shown in figure 9(i). The circuit signals are transmitted through SWNT-based bit/word bus lines. The resulting circuit can be mounted on an arbitrary curved surface and can be further applied on the arm or the joint of a robot [55].

6. Conclusion

This article presents an overview of the various technologies and materials that have been used for stretchable interconnects. In particular, our focus has been on printable nanocomposites as they enable systems with intrinsic stretchability and excellent electrical conductivity. With innovative designs these interconnect structures could allow electronic systems to withstand strain up to 200%. By incorporating intrinsic and stretchable materials, the tolerable strain can be even larger. Among the various materials, rubber-like nanocomposites draw major attention because of their high electrical performance and softness. The filler-polymer matrix system is summarized according to the filler materials, which includes carbon-based and metal-based fillers. Due to the difference in the morphology, size, and electrical conductivity of dispersed fillers, the trends in percolation ratio, maximum electrical conductivity and elastic modulus of resultant nanocomposites between carbon-based and metal-based nanocomposites exhibit different behaviors. In general, high aspect ratio NWs are preferred as fillers for nanocomposites as they allow one to maintain a low electrical percolation threshold and high stretchability. Compared with metal-based fillers, carbon-based fillers have advantages in terms of low cost and less degradation (oxidation, etc) during processing. If metal-based fillers are dealt with carefully, they can be more suitable for stretchable interconnect applications. The in-depth analysis of printed nanocomposite-based stretchable interconnects presented in this paper will offer an excellent guide for researchers in this field and flexible electronics in general.

Acknowledgments

This work was supported by the European Commission under grant agreement PITN-GA-2012-317488-CONTEST and Engineering and Physical Sciences Council (EPSRC) Fellowship for Growth—Printable Tactile Skin (EP/M002527/1).

References

[1] Kim D-H *et al* 2011 Materials for multifunctional balloon catheters with capabilities in cardiac electrophysiological mapping and ablation therapy *Nat. Mater.* **10** 316–23
[2] Son D *et al* 2014 Multifunctional wearable devices for diagnosis and therapy of movement disorders *Nat. Nanotechnol.* **9** 397–404
[3] Sekitani T, Nakajima H, Maeda H, Fukushima T, Aida T, Hata K and Someya T 2009 Stretchable active-matrix organic light-emitting diode display using printable elastic conductors *Nat. Mater.* **8** 494–9
[4] Sekitani T and Someya T 2012 Stretchable organic integrated circuits for large-area electronic skin surfaces *MRS Bull.* **37** 236–45
[5] Dahiya R, Navaraj W T, Khan S and Polat E O 2015 Developing electronic skin with the sense of touch *Inf. Disp.* **31** 6–10 http://informationdisplay.org/IDArchive/2015/JulyAugust/FrontlineTechnologyElectronicSkin.aspx
[6] Yogeswaran N *et al* 2015 New materials and advances in making electronic skin for interactive robots *Adv. Robot.* **29** 1359–73
[7] Dahiya R S, Mittendorfer P, Valle M, Cheng G and Lumelsky V J 2013 Directions toward effective utilization of tactile skin: a review *IEEE Sens. J.* **13** 4121–38
[8] Dahiya R S, Metta G, Valle M and Sandini G 2010 Tactile Sensing—from humans to humanoids *IEEE Trans. Robot.* **26** 1–20
[9] Gupta S, Heidari H, Vilouras A, Lorenzelli L and Dahiya R 2016 Device modelling for bendable piezoelectric fet-based touch sensing system *IEEE Trans. Circuits Syst. I* **63** 2200–8
[10] Dahiya R S and Valle M 2013 *Robotic Tactile Sensing: Technologies and System* (Dordrecht: Springer Science & Business Media) pp 1–248 ISBN 978-94-007-0579-1
[11] Sun Y, Choi W M, Jiang H, Huang Y Y and Rogers J A 2006 Controlled buckling of semiconductor nanoribbons for stretchable electronics *Nat. Nanotechnol.* **1** 201–7
[12] Dahiya R, Gottardi G and Laidani N 2015 PDMS residues-free micro/macrostructures on flexible substrates *Microelectron. Eng.* **136** 57–62
[13] Dahiya R S, Adami A, Collini C and Lorenzelli L 2012 Fabrication of single crystal silicon micro-/nanostructures and transferring them to flexible substrates *Microelectron. Eng.* **98** 502–7
[14] Shakthivel D, Núñez C G and Dahiya R 2016 *Inorganic Semiconducting Nanowires for Flexible Electronics* (USA: United Scholars Publication) ISBN-13: 978-0692751718
[15] Choi W M, Song J, Khang D-Y, Jiang H, Huang Y Y and Rogers J A 2007 Biaxially stretchable 'wavy' silicon nanomembranes *Nano Lett.* **7** 1655–63
[16] Dahiya R S and Gennaro S 2013 Bendable ultra-thin chips on flexible foils *IEEE Sens. J.* **13** 4030–7
[17] Hammock M L, Chortos A, Tee B C K, Tok J B H and Bao Z 2013 25th anniversary article: the evolution of electronic skin (E-Skin): a brief history, design considerations, and recent progress *Adv. Mater.* **25** 5997–6038
[18] Benight S J, Wang C, Tok J B H and Bao Z 2013 Stretchable and self-healing polymers and devices for electronic skin *Prog. Polym. Sci.* **38** 1961–77
[19] Rogers J A 2014 Materials for semiconductor devices that can bend, fold, twist, and stretch *MRS Bull.* **39** 549–56
[20] Kim D-H, Lu N, Huang Y and Rogers J A 2012 Materials for stretchable electronics in bioinspired and biointegrated devices *MRS Bull.* **37** 226–35
[21] Rogers J A, Someya T and Huang Y 2010 Materials and mechanics for stretchable electronics *Science* **327** 1603–7
[22] Lu N and Yang S 2015 Mechanics for stretchable sensors *Curr. Opin. Solid State Mater. Sci.* **19** 149–59
[23] Hocheng H and Chen C-M 2014 Design, fabrication and failure analysis of stretchable electrical routings *Sensors (Basel)* **14** 11855–77
[24] Yao S and Zhu Y 2015 Nanomaterial-enabled stretchable conductors: strategies, materials and devices *Adv. Mater.* **27** 1480–511
[25] Bauhofer W and Kovacs J Z 2009 A review and analysis of electrical percolation in carbon nanotube polymer composites *Compos. Sci. Technol.* **69** 1486–98
[26] Mann A E, Dubey M B, Martin W, Ralph E L, Oliver R L and Saul S 1963 Solar cell system US 3094439 Patent: US3094439 A https://www.google.com/patents/US3094439

[27] Kim R-H *et al* 2010 Waterproof AlInGaP optoelectronics on stretchable substrates with applications in biomedicine and robotics *Nat. Mater.* **9** 929–37
[28] Pylatiuk C, Kargov A and Schulz S 2006 Design and evaluation of a low-cost force feedback system for myoelectric prosthetic hands *JPO J. Prosthetics Orthot.* **18** 57–61
[29] Hussain A M, Ghaffar F A, Park S I, Rogers J A, Shamim A and Hussain M M 2015 Metal/polymer based stretchable antenna for constant frequency far-field communication in wearable electronics *Adv. Funct. Mater.* **25** 6565–75
[30] Yoshikai T, Fukushima H, Hayashi M and Inaba M 2009 Development of soft stretchable knit sensor for humanoids' whole-body tactile sensibility *9th IEEE-RAS Int. Conf. on Humanoid Robots, HUMANOIDS09* pp 624–31
[31] Chen Y, Yu M, Bruck H A and Smela E 2016 Stretchable touch-sensing skin over padding for co-robots *Smart Mater. Struct.* **25** 055006
[32] Xu L *et al* 2014 3D multifunctional integumentary membranes for spatiotemporal cardiac measurements and stimulation across the entire epicardium *Nat. Commun.* **5** 3329
[33] Guo L, Ma M, Zhang N, Langer R and Anderson D G 2014 Stretchable polymeric multielectrode array for conformal neural interfacing *Adv. Mater.* **26** 1427–33
[34] Dahiya R S 2015 Epidermal electronics—flexible electronics for biomedical applications *Handbook of Bioelectronics* ed S Carrara and K Iniewski (Cambridge University Press) pp 245–55
[35] Polat E O, Balci O, Kakenov N, Uzlu H B, Kocabas C and Dahiya R 2015 Synthesis of large area graphene for high performance in flexible optoelectronic devices *Nat. Publ. Gr.* **5** 1–10
[36] Ge J, Sun L, Zhang F R, Zhang Y, Shi L A, Zhao H Y, Zhu H W, Jiang H L and Yu S H 2016 A stretchable electronic fabric artificial skin with pressure-, lateral strain-, and flexion-sensitive properties *Adv. Mater.* **28** 722–8
[37] Cheng M-Y, Tsao C-M, Lai Y-Z and Yang Y-J 2011 The development of a highly twistable tactile sensing array with stretchable helical electrodes *Sensors Actuators A Phys.* **166** 226–33
[38] Cheng M Y, Tsao C M and Yang Y J 2010 An anthropomorphic robotic skin using highly twistable tactile sensing array *Proc. 2010 5th IEEE Conf. Ind. Electron. Appl. ICIEA 2010* pp 650–5
[39] Bonderover E and Wagner S 2004 A woven inverter circuit for e-textile applications *IEEE Electron Device Lett.* **25** 295–7
[40] Hamedi M, Forchheimer R and Inganäs O 2007 Towards woven logic from organic electronic fibres *Nat. Mater.* **6** 357–62
[41] Hoshi T and Shinoda H 2006 Robot skin based on touch-area-sensitive tactile element *Proc.—IEEE Int. Conf. Robot. Autom.* **2006** 3463–8
[42] Huyghe B, Rogier H, Vanfleteren J and Axisa F 2008 Design and manufacturing of stretchable high-frequency interconnects *IEEE Trans. Adv. Packag.* **31** 802–8
[43] Brosteaux D, Gonzalez M and Vanfleteren J 2007 Design and fabrication of elastic interconnections for stretchable electronic circuits *IEEE Electron Device Lett.* **28** 552–4
[44] Verplancke R, Bossuyt F, Cuypers D and Vanfleteren J 2012 Thin-film stretchable electronics technology based on meandering interconnections: fabrication and mechanical performance *J. Micromech. Microeng.* **22** 015002
[45] Kim D-H, Liu Z, Kim Y-S, Wu J, Song J, Kim H-S, Huang Y, Hwang K-C, Zhang Y and Rogers J A 2009 Optimized structural designs for stretchable silicon integrated circuits *Small* **5** 2841–7
[46] Lacour S P, Jones J, Wagner S, Li T and Suo Z 2005 Stretchable interconnects for elastic electronic surfaces *Proc. IEEE* **93** 1459–67
[47] Rogers J, Huang Y, Schmidt O G and Gracias D H 2016 Origami MEMS and NEMS *MRS Bull.* **41** 123–9
[48] Khang D-Y, Jiang H, Huang Y and Rogers J A 2006 A stretchable form of single crystal silicon for high performance electronics on rubber substrates *Science* **311** 208–12
[49] Lee H, Bae C, Duy L T, Sohn I, Kim D, Song Y, Kim Y and Lee N 2016 Mogul-patterned elastomeric substrate for stretchable electronics *Adv. Mater.* **28** 3069–77
[50] Yu Y, Zeng J, Chen C, Xie Z, Guo R, Liu Z, Zhou X, Yang Y and Zheng Z 2014 Three-dimensional compressible and stretchable conductive composites *Adv. Mater.* **26** 810–5
[51] Gui X, Cao A, Wei J, Li H, Jia Y, Li Z, Fan L, Wang K, Zhu H and Wu D 2010 Soft, highly conductive nanotube compressibility *ACS Nano* **4** 2320–6
[52] Chen Z, Ren W, Gao L, Liu B, Pei S and Cheng H-M 2011 Three-dimensional flexible and conductive interconnected graphene networks grown by chemical vapour deposition *Nat. Mater.* **10** 424–8
[53] Guo C F, Sun T, Liu Q, Suo Z and Ren Z 2014 Highly stretchable and transparent nanomesh electrodes made by grain boundary lithography *Nat. Commun.* **5**
[54] Bagal A, Dandley E C, Zhao J, Zhang X A, Oldham C J, Parsons G N and Chang C-H 2015 Multifunctional nano-accordion structures for stretchable transparent conductors *Mater. Horizons* **2** 486–94
[55] Sekitani T, Noguchi Y, Hata K, Fukushima T, Aida T and Someya T 2008 A rubberlike stretchable active matrix using elastic conductors *Science (80-.).* **321** 1468–73
[56] Zhang Y, Sheehan C J, Zhai J, Zou G, Luo H, Xiong J, Zhu Y T and Jia Q X 2010 Polymer-embedded carbon nanotube ribbons for stretchable conductors *Adv. Mater.* **22** 3027–31
[57] Khan S, Dang W, Lorenzelli L and Dahiya R 2015 Flexible pressure sensors based on screen-printed P(VDF-TrFE) and P(VDF-TrFE)/MWCNTs *IEEE Trans. Semicond. Manuf.* **28** 486–93
[58] Dang W, Khan S, Lorenzelli L, Vinciguerra V and Dahiya R 2015 Stretchable interconnects using screen printed nanocomposites of MWCNTs with PDMS and P(VDF-TrFE) *IEEE PRIME* (https://doi.org/10.1109/PRIME.2015.7251381)
[59] Noda K, Iwase E, Matsumoto K and Shimoyama I 2010 Stretchable liquid tactile sensor for robot-joints *IEEE Int. Conf. on Robotics and Automation* pp 4212–7
[60] Khan S, Tinku S, Lorenzelli L and Dahiya R S 2015 Flexible tactile sensors using screen-printed P(VDF-TrFE) and MWCNT/PDMS composites *IEEE Sens. J.* **15** 3146–55
[61] Liu C-X and Choi J-W 2009 Patterning conductive PDMS nanocomposite in an elastomer using microcontact printing *J. Micromech. Microeng.* **19** 085019
[62] Sangwan V K, Ballarotto V W, Hines D R, Fuhrer M S and Williams E D 2010 Controlled growth, patterning and placement of carbon nanotube thin films *Solid. State. Electron.* **54** 1204–10
[63] Abdelhalim A, Abdellah A, Scarpa G and Lugli P 2013 Fabrication of carbon nanotube thin films on flexible substrates by spray deposition and transfer printing *Carbon N. Y* **61** 72–9
[64] Béduer A, Seichepine F, Flahaut E and Vieu C 2012 A simple and versatile micro contact printing method for generating carbon nanotubes patterns on various substrates *Microelectron. Eng.* **97** 301–5
[65] Khan S, Member L L, Dahiya R and Member S 2016 Flexible MISFET devices from transfer printed si microwires and spray coating *J. Electron Devices Soc.* **4** 189–96
[66] Khan S, Yogeswaran N, Taube W, Lorenzelli L and Dahiya R 2015 Flexible FETs using ultrathin Si microwires embedded in solution processed dielectric and metal layers *J. Micromech. Microeng.* **25** 125019
[67] Zhuang J-L, Ar D, Yu X-J, Liu J-X and Terfort A 2013 Patterned deposition of metal-organic frameworks onto plastic, paper, and textile substrates by inkjet printing of a precursor solution *Adv. Mater.* **25** 4631–5

[68] Minemawari H, Yamada T, Matsui H, Tsutsumi J, Haas S, Chiba R, Kumai R and Hasegawa T 2011 Inkjet printing of single-crystal films *Nature* **475** 364–7
[69] Soukup R, Hamáček A and Řeboun J 2012 Organic based sensors: Novel screen printing technique for sensing layers deposition *Proc. Int. Spring Semin. Electron. Technol.* pp 19–24
[70] Jabbour G E, Radspinner R and Peyghambarian N 2001 Screen printing for the fabrication of organic light-emitting devices *IEEE J. Sel. Top. Quantum Electron.* **7** 769–73
[71] Liang J, Tong K and Pei Q 2016 A water-based silver-nanowire screen-print ink for the fabrication of stretchable conductors and wearable thin-film transistors *Adv. Mater.* **28** 5986–96
[72] Hess-Dunning A E, Tyler D J and Zorman C A 2013 Stretchable thin-film metal structures on a stimuli-responsive polymer nanocomposite for mechanically-dynamic microsystems *Transducers 2013 (Barcelona, SPAIN)* pp 2229–32
[73] Stoyanov H, Kollosche M, Risse S, Waché R and Kofod G 2013 Soft conductive elastomer materials for stretchable electronics and voltage controlled artificial muscles *Adv. Mater.* **25** 578–83
[74] Lipomi D J, Lee J A, Vosgueritchian M, Tee B C-K, Bolander J A and Bao Z 2012 Electronic properties of transparent conductive films of PEDOT:PSS on stretchable substrates *Chem. Mater.* **24** 373–82
[75] Alemu D, Wei H-Y, Ho K-C and Chu C-W 2012 Highly conductive PEDOT:PSS electrode by simple film treatment with methanol for ITO-free polymer solar cells *Energy Environ. Sci.* **5** 9662
[76] Kim Y H, Sachse C, Machala M L, May C, Müller-Meskamp L and Leo K 2011 Highly conductive PEDOT:PSS electrode with optimized solvent and thermal post-treatment for ITO-free organic solar cells *Adv. Funct. Mater.* **21** 1076–81
[77] Takano T, Masunaga H, Fujiwara A, Okuzaki H and Sasaki T 2012 PEDOT nanocrystal in highly conductive PEDOT:PSS polymer films *Macromolecules* **45** 3859–65
[78] Timpanaro S, Kemerink M, Touwslager F J, De Kok M M and Schrader S 2004 Morphology and conductivity of PEDOT/PSS films studied by scanning-tunneling microscopy *Chem. Phys. Lett.* **394** 339–43
[79] Cho C K, Hwang W J, Eun K, Choa S H, Na S I and Kim H K 2011 Mechanical flexibility of transparent PEDOT:PSS electrodes prepared by gravure printing for flexible organic solar cells *Sol. Energy Mater. Sol. Cells* **95** 3269–75
[80] Larson C *et al* 2016 Highly stretchable electroluminescent skin for optical signaling and tactile sensing *Science* **351** 1071–4
[81] Kim S, Lee J and Choi B 2015 Stretching and twisting sensing with liquid-metal strain gauges printed on silicone elastomers *IEEE Sens. J.* **15** 6077–8
[82] Ladd C, So J H, Muth J and Dickey M D 2013 3D printing of free standing liquid metal microstructures *Adv. Mater.* **25** 5081–5
[83] Choi S *et al* 2015 Stretchable heater using ligand-exchanged silver nanowire nanocomposite for wearable articular thermotherapy *ACS Nano* **9** 6626–33
[84] Suikkola J, Björninen T, Mosallaei M, Kankkunen T, Iso-ketola P, Ukkonen L, Vanhala J and Mäntysalo M 2016 Screen-printing fabrication and characterization of stretchable electronics *Sci. Rep.* 1–8
[85] Liu C-X and Choi J-W 2012 Improved dispersion of carbon nanotubes in polymers at high concentrations *Nanomater.* **2** 329–47
[86] De S and Coleman J N 2011 The effects of percolation in nanostructured transparent conductors *MRS Bull.* **36** 774–81
[87] Kumar S, Murthy J Y and Alam M A 2005 Percolating conduction in finite nanotube networks *Phys. Rev. Lett.* **95** 066802
[88] Jack D A, Yeh C-S, Liang Z, Li S, Park J G and Fielding J C 2010 Electrical conductivity modeling and experimental study of densely packed SWCNT networks *Nanotechnology* **21** 195703
[89] Colasanti S, Bhatt V D and Lugli P 2014 3D modeling of CNT networks for sensing applications *IEEE*
[90] Balberg I 2009 Tunnelling and percolation in lattices and the continuum *J. Phys. D: Appl. Phys.* **42** 64003
[91] Zheng X, Forest M G, Vaia R, Arlen M and Zhou R 2007 A strategy for dimensional percolation in sheared nanorod dispersions *Adv. Mater.* **19** 4038–43
[92] Bao W S, Meguid S A, Zhu Z H and Weng G J 2012 Tunneling resistance and its effect on the electrical conductivity of carbon nanotube nanocomposites *J. Appl. Phys.* **111** 93726
[93] Halpin J C and Kardos J L 1976 The Halpin-Tsai equations: a review *Polym. Eng. Sci.* **16** 344–52
[94] Nielsen L E 1970 Generalized equation for the elastic moduli of composite materials *J. Appl. Phys.* **41** 4626–7
[95] Li L and Chung D D 1991 Electrically conducting powder filled polyimidesiloxane *Composites* **22** 211–8
[96] Jung H, Moon J, Baek D, Lee J, Choi Y and Hong J 2012 CNT/PDMS composite flexible dry electrodes for long-term ECG monitoring *IEEE Trans. Biomed. Eng.* **59** 1472–9
[97] Hou Y, Wang D, Zhang X-M, Zhao H, Zha J-W and Dang Z-M 2013 Positive piezoresistive behavior of electrically conductive alkyl-functionalized graphene/polydimethylsilicone nanocomposites *J. Mater. Chem.* C **1** 515–21
[98] Shih W-P, Tsao L-C, Lee C-W, Cheng M-Y, Chang C, Yang Y-J and Fan K-C 2010 Flexible temperature sensor array based on a graphite-polydimethylsiloxane composite *Sensors (Basel)* **10** 3597–610
[99] Celzard A, McRae E, Marêché J F, Furdin G and Sundqvist B 1998 Conduction mechanisms in some graphite–polymer composites: effects of temperature and hydrostatic pressure *J. Appl. Phys.* **83** 1410
[100] Serra N, Maedera T, Lemaire P and Ryser P 2009 Formulation of composite resistive pastes for micro-heater manufacturing *Procedia Chem.* **1** 48–51
[101] Mathur R B, Dhakate S R, Gupta D K, Dhami T L and Aggarwal R K 2008 Effect of different carbon fillers on the properties of graphite composite bipolar plate *J. Mater. Process. Technol.* **203** 184–92
[102] Mironov V S, Kim J K, Park M Ã, Lim S and Cho W K 2007 Comparison of electrical conductivity data obtained by four-electrode and four-point probe methods for graphite-based polymer composites *Polym. Test.* **26** 547–55
[103] Nagata K, Iwabuki H and Nigo H 1998 Effect of particle size of graphites on electrical conductivity of graphite/polymer composite *Compos. Interfaces* **6** 483–95
[104] Du X S, Xiao M and Meng Y Z 2004 Synthesis and characterization of polyaniline/graphite conducting nanocomposites *J. Polym. Sci. Part B Polym. Phys.* **42** 1972–8
[105] Fim F D C, Guterres J M, Basso N R S and Galland G B 2010 Polyethylene/graphite nanocomposites obtained by *in situ* polymerization *J. Polym. Sci. Part A Polym. Chem.* **48** 692–8
[106] Chen G, Wang H and Zhao W 2008 Fabrication of highly ordered polymer/graphite flake composite with eminent anisotropic electrical property *Polym. Adv. Technol.* **19** 1113–7
[107] Khosla A and Gray B L 2009 Preparation, characterization and micromolding of multi-walled carbon nanotube polydimethylsiloxane conducting nanocomposite polymer *Mater. Lett.* **63** 1203–6
[108] Lee J-B and Khang D-Y 2012 Electrical and mechanical characterization of stretchable multi-walled carbon nanotubes/polydimethylsiloxane elastomeric composite conductors *Compos. Sci. Technol.* **72** 1257–63
[109] Lu J, Lu M, Bermak A, Member S and Lee Y 2007 Study of piezoresistance effect of carbon nanotube-PDMS composite materials for nanosensors *7th IEEE Int. Conf. on Nanotechnology* pp 1240–3
[110] Špírková M, Duszová A, Pore R, Kredatusová J, Bureš R, Fáberová M and Šlouf M 2014 Thermoplastic polybutadiene-based polyurethane/carbon nanofiber composites *Compos. Part* B **67** 434–40

[111] Moreno I, Navascues N, Arruebo M, Irusta S and Santamaria J 2013 Facile preparation of transparent and conductive polymer films based on silver nanowire/polycarbonate nanocomposites *Nanotechnology* **24** 275603
[112] Chen S-P and Liao Y-C 2014 Highly stretchable and conductive silver nanowire thin films formed by soldering nanomesh junctions *Phys. Chem. Chem. Phys.* **16** 19856–60
[113] Lee P *et al* 2014 Highly stretchable or transparent conductor fabrication by a hierarchical multiscale hybrid nanocomposite *Adv. Funct. Mater.* **24** 5671–8
[114] Lee M S *et al* 2013 High-performance, transparent, and stretchable electrodes using graphene-metal nanowire hybrid structures *Nano Lett.* **13** 2814–21
[115] Araki T, Nogi M, Suganuma K, Kogure M and Kirihara O 2011 Printable and stretchable conductive wirings comprising silver flakes and elastomers *IEEE Electron Device Lett.* **32** 1424–6
[116] Hu W, Niu X, Li L, Yun S, Yu Z and Pei Q 2012 Intrinsically stretchable transparent electrodes based on silver-nanowire–crosslinked-polyacrylate composites *Nanotechnology* **23** 344002
[117] Larmagnac A, Eggenberger S, Janossy H and Vörös J 2014 Stretchable electronics based on Ag-PDMS composites *Sci. Rep.* **4** 7254
[118] Martinez V, Stauffer F, Adagunodo M O, Forro C, Vörös J and Larmagnac A 2015 Stretchable silver nanowire–elastomer composite microelectrodes with tailored electrical properties *ACS Appl. Mater. Interfaces* **7** 13467–75
[119] Song L, Myers A C, Adams J J and Zhu Y 2014 Stretchable and reversibly deformable radio frequency antennas based on silver nanowires *ACS Appl. Mater. Interfaces* **6** 4248–53
[120] Tybrandt K, Stauffer F and Vörös J 2016 Multilayer patterning of high resolution intrinsically stretchable electronics *Nat. Publ. Gr.* **6** 1–14
[121] Xu F and Zhu Y 2012 Highly conductive and stretchable silver nanowire conductors *Adv. Mater.* **24** 5117–22
[122] Kim K K, Hong S, Cho H M, Lee J, Suh Y D, Ham J and Ko S H 2015 Highly sensitive and stretchable multidimensional strain sensor with prestrained anisotropic metal nanowire percolation networks *Nano Lett.* **15** 5240–7
[123] Yun S, Niu X, Yu Z, Hu W, Brochu P and Pei Q 2012 Compliant silver nanowire-polymer composite electrodes for bistable large strain actuation *Adv. Mater.* **24** 1321–7
[124] Doganay D, Coskun S, Kaynak C and Unalan H E 2016 Electrical, mechanical and thermal properties of aligned silver nanowire/polylactide nanocomposite films *Compos. Part* B **99** 288–96
[125] Xu W, Xu Q, Huang Q, Tan R, Shen W and Song W 2015 Electrically conductive silver nanowires-filled methylcellulose composite transparent films with high mechanical properties *Mater. Lett.* **152** 173–6
[126] Narayanan S, Hajzus J R, Treacy C E, Bockstaller M R and Porter L M 2014 Polymer embedded silver-nanowire network structures—a platform for the facile fabrication of flexible transparent conductors *ECS J. Solid State Sci. Technol.* **3** P363–9
[127] Lee J, Lee P, Lee H B, Hong S, Lee I, Yeo J, Lee S S, Kim T S, Lee D and Ko S H 2013 Room-temperature nanosoldering of a very long metal nanowire network by conducting-polymer-assisted joining for a flexible touch-panel application *Adv. Funct. Mater.* **23** 4171–6
[128] Cortes L Q, Lonjon A, Dantras E and Lacabanne C 2014 High-performance thermoplastic composites poly(ether ketone ketone)/silver nanowires: morphological, mechanical and electrical properties *J. Non. Cryst. Solids* **391** 106–11
[129] Lonjon A, Caffrey I, Carponcin D, Dantras E and Lacabanne C 2013 High electrically conductive composites of Polyamide 11 filled with silver nanowires: nanocomposites processing, mechanical and electrical analysis *J. Non. Cryst. Solids* **376** 199–204
[130] Sureshkumar M, Na H Y, Ahn K H and Lee S J 2015 Conductive nanocomposites based on polystyrene microspheres and silver nanowires by latex blending *ACS Appl. Mater. Interfaces* **7** 756–64
[131] Tang Y, Gong S, Chen Y, Yap L W and Cheng W 2014 Manufacturable conducting rubber ambers and stretchable conductors from copper nanowire aerogel monoliths *ACS Nano* **8** 5707–14
[132] Im H, Jung S, Jin J, Lee D, Lee J, Lee D and Lee J 2014 Flexible transparent conducting hybrid film using a surface-embedded copper nanowire network : a highly oxidation-resistant copper nanowire electrode for flexible optoelectronics *ACS Nano* **8** 10973–9
[133] Gelves G A, Lin B, Sundararaj U and Haber J A 2006 Low electrical percolation threshold of silver and copper nanowires in polystyrene composites *Adv. Funct. Mater.* **16** 2423–30
[134] An B W, Gwak E J, Kim K, Kim Y C, Jang J, Kim J Y and Park J U 2016 Stretchable, transparent electrodes as wearable heaters using nanotrough networks of metallic glasses with superior mechanical properties and thermal stability *Nano Lett.* **16** 471–8
[135] Lonjon A, Laffont L, Demont P, Dantras E and Lacabanne C 2009 New highly conductive nickel nanowire-filled P (VDF-TrFE) copolymer nanocomposites : elaboration and structural study *J. Phys. Chem.* C **113** 12002–6
[136] Lonjon A, Laffont L, Demont P, Dantras E and Lacabanne C 2010 Structural and electrical properties of gold nanowires/P (VDF-TrFE) nanocomposites *J. Phys. D: Appl. Phys.* **43** 345401
[137] Kim J *et al* 2014 Stretchable silicon nanoribbon electronics for skin prosthesis *Nat. Commun.* **5** 5747
[138] Webb R C *et al* 2013 Ultrathin conformal devices for precise and continuous thermal characterization of human skin *Nat. Mater.* **12** 938–44
[139] Yamada T, Hayamizu Y, Yamamoto Y, Yomogida Y, Izadi-Najafabadi A, Futaba D N and Hata K 2011 A stretchable carbon nanotube strain sensor for human-motion detection *Nat. Nanotechnol.* **6** 296–301
[140] Gao W *et al* 2016 Fully integrated wearable sensor arrays for multiplexed *in situ* perspiration analysis *Nature* **529** 509–14
[141] Huang X, Liu Y, Chen K, Shin W J, Lu C J, Kong G W, Patnaik D, Lee S H, Cortes J F and Rogers J A 2014 Stretchable, wireless sensors and functional substrates for epidermal characterization of sweat *Small* **10** 3083–90
[142] Park S-I *et al* 2009 Printed assemblies of inorganic light-emitting diodes for deformable and semitransparent displays *Science* **325** 977–81
[143] Xu S *et al* 2014 Soft microfluidic assemblies of sensors, circuits, and radios for the skin *Science* **344** 70–4
[144] Da Silva A B, Marini J, Gelves G, Sundararaj U, Gregório R and Bretas R E S 2013 Synergic effect in electrical conductivity using a combination of two fillers in PVDF hybrids composites *Eur. Polym. J.* **49** 3318–27
[145] Moreno I, Navascues N, Irusta S and Santamaria J 2012 Silver nanowires/polycarbonate composites for conductive films *IOP Conf. Ser.: Mater. Sci. Eng.* **40** 1–6